공학석사학위논문

Conjugation of CD40-binding peptide to glycol chitosan nanoparticle for localized delivery of tumor microenvironment modulator

종양미세환경 조절인자의 국소적 전달을 위한

펩타이드 글라이콜 키토산 나노입자 결합체 연구

2017년 2월

서울대학교 대학원

협동과정 바이오엔지니어링전공

김 소 정

Conjugation of CD40-binding peptide to glycol chitosan nanoparticle for localized delivery of tumor microenvironment modulator

종양미세환경 조절인자의 국소적 전달을 위한 펩타이드 글라이콜 키토산 나노입자 결합체 연구

지도 교수 김병수

이 논문을 공학석사학위논문으로 제출함

2017년 2월

서울대학교 대학원
협동과정 바이오엔지니어링전공

김 소 정

김소정의 석사 학위논문을 인준함
2017년 2월

위 원 장 황 석 연 (인)
부 위 원 장 김 병 수 (인)
위 원 한 지 숙 (인)

Abstract

Conjugation of CD40-binding peptide to glycol chitosan nanoparticle for localized delivery of tumor microenvironment modulator

Sojeong Kim

Interdisciplinary Program for Bioengineering

The Graduate School

Seoul National University

Cancer immunotherapy focuses on helping the immune system fight and control cancer and has rapidly progressed in the recent years. Agonistic CD40 monoclonal antibodies have been proposed as a new therapeutic method that enhances anticancer immunity by various mechanisms that alter the immune-suppressive tumor microenvironment. Previous researches have shown that CD40 binding not only causes tumor cell death but also activates macrophages to rapidly penetrate tumors, become tumoricidal and promote the reduction of tumor stroma. In this study, in order to avoid unwanted systemic side effects while maintaining

the anti-tumor effects of CD40 antibody, localized delivery of agonistic CD40-binding peptide (CD40p) that mimics a portion of human CD40 ligand was achieved by conjugating CD40p to hydrophobically modified glycol chitosan nanoparticles (CD40p-CNP). The immunomodulatory nanoparticles showed cytotoxicity against human cancer cells and enhanced phagocytic activity of macrophages *in vitro*. Systemic injection of CD40p-CNP into tumor-bearing mice resulted in tumor-targeted delivery and significant inhibition of tumor growth that was similar to the effect of local injection of CD40p. Also, the potential of localized cancer immunotherapy via CD40-dependent mechanism that targets tumor stroma in the treatment of cancer was demonstrated. The primary findings of this study provide a new platform to treat cancer through localized delivery of immunotherapeutic agents via systemic injection of nanoparticle which can also be combined with other treatment modalities to facilitate its effect.

Keywords : : cancer immunotherapy, CD40 binding peptide, CD40 antibody, glycol chitosan nanoparticle, tumor microenvironment, tumor-infiltrated lymphocytes, tumor growth inhibition

Student Number : 2015-21210

Table of Contents

List of Tables

List of Figures

Figure 8. *In vitro* activation of differentiated THP-1. (A) Differentiation of THP-1 confirmed by FACS analysis. (B) Microscopic images of differentiated THP-1 after treatments. Red arrows indicate activated macrophages. Original magnification power was 400x. (C) Molecular changes of p-p38 / p38 and (D) Interluekin-12 (IL-12) / beta-actin in differentiated THP-1 following the treatments analyzed by Western blot.

Figure 9. *In vitro* phagocytic activity of differentiated THP-1 after co-culture with U87 for 2 h. (A) Enlarged image of THP-1macrophages undergoing phagocytosis. (B) Total microscopic images of macrophages after co-culture. Red arrows indicate phagocytosis of cancer cells into macrophages. Original magnification power was 400x. (C) Number of macrophages undergoing phagocytosis manually counted from the microscopic images (n=5) and (D) analyzed by flow cytometry. (E) Molecular changes in differentiated THP-1 after treatments and co-culture analyzed by Western blot.

Figure 10. Time-dependent tumor accumulation of CNP, CD40p-CNP, and CD40p after intravenous injection. (A) *In vivo* tumor NIRF images of B16F10 tumor-bearing mice over time after nanoparticle/peptide injection. (B) *Ex vivo* NIRF images of tumors. (C) Total amount of fluorescence intensity in the tumors excised from the mice at 48 h after injection.

Figure 11. Effect of localized injection of CD40p or intravenous injection CD40p-CNP on the inhibition of tumor growth. (A) Timeline of the experiment (B) Measurements of the tumor volumes over time (C) Percentage of increase in tumor volumes after final treatments compared to the initial tumor volumes. (D) Molecular changes of p-p38 / p38 in tumor lysates from mouse tumor xenograft models after designed treatments.

Figure 12. Histological analysis of the tumor tissues after the treatments with CD40p (I.T.), CD40p-CNP (I.V.), or PBS**.** (A) H&E staining (B) Anti-CD68 IHC staining against macrophages (brown) in the tumor tissues.

1. Introduction

Recently, the importance of cancer immunotherapy that uses a patient's own immune system to help fight cancer has been highlighted in comparison to other treatments, such as surgery, chemotherapy, and radiation therapy **[1, 2]**. It is due to the various problems that standard cancer treatments have often caused: temporary tumor regressions, severe toxicity, and side effects that include drug tolerance, damaged healthy cells, exposure to radiation, and fatigue. On the other hand, cancer immunotherapy focuses on using the body's own immune cells to fight against cancer cells for non-toxic cancer treatments with a lower chance of severe side effects. Various strategies of cancer immunotherapy include vaccination, adoptive T cell therapy, and antibody-mediated therapy. Currently, the number of studies that are approved by the FDA or that entered into the clinical trials are rapidly increasing, reflecting the huge attention and the activeness of the researches in the field **[3]**.

Most cancer immunotherapy targets tumor and its microenvironment (TME). TME is developed in complex tissue environments with tumor cells, immune cells, endothelial cells, and connective tissue cells. It also possesses infiltrating cells, such as macrophages, dendritic cells (DC), and lymphocytes. Tumor cells become malignant and metastatic by the secretion of specific chemokines, such as VEGF, GM-CSF, G-CSF, and gangliosides. They also suppress the immune cells nearby to lose their function. For examples, tumor-infiltrated regulatory T cells (Treg) secrete immune-suppressive cytokine such as IL-10 and suppress activation of cytotoxic T lymphocyte. Maturation of dendritic cells are also suppressed to reduce antigen presentation **[4]**. Tumor-associated macrophages acquire M2-like phenotype that induces anti-inflammation **[4, 5]**.

CD40 is a co-stimulatory TNF receptor superfamily member which is expressed on immune cells, such as macrophages, B cells, dendritic cells, as well as tumor cells and non-immune cells **[6, 7]**. Binding of CD40 and its ligand is required for the activation of the immune cells. Specifically, CD40 binding is used by T helper cells to stimulate other immune cells such as antigen-presenting cells for pro-inflammatory responses. CD40 binding mechanism can be especially useful in overcoming the immune-suppressive TME **[8-10]**. Firstly, dendritic cells bound with CD40 ligand are activated and present tumor-associated antigens on the surface. Cytotoxic T cells recognize the tumor-associated antigens on the surface of the activated dendritic cells and remove the tumor cells that express the same tumor-associated antigens. Secondly, CD40 binding to macrophages induces activation of M0-type macrophages and re-education or re-polarization of immunosuppressive M2-type tumor-associated macrophages to become more cytotoxic towards tumor cells. Thirdly, CD40 receptor binding to tumor cells has direct tumoricidal effect, which not only induces death of the tumor cells that express CD40 receptors, but also contributes to producing more tumor-associated antigens to further stimulate the antigen-presenting cells **[11, 12]**. Most relevant studies have focused on dendritic cells and tumor cells **[13-18]**, but macrophages possess the potential to directly kill tumor cells more efficiently and to revert the immunosuppressive characteristic of TME **[19-21]**. More research on the effect of CD40 binding on macrophages may lead to better understanding of the mechanism for overcoming TME.

Although conventional approaches commonly involve systemic administration of immunotherapeutic agents, in order to reduce the side effects associated with systemic injection, localized therapy has been studied by many researchers. Local injection is also effective in overcoming immunosuppressive factors of the TME to promote the immune-induced destruction. Local immunotherapy of CD40 has shown especially promising results **[16, 22, 23]**.

However, local injections are oftentimes difficult to achieve due to the location or dispersive nature of some tumors, such as melanoma, glioblastoma, and pancreatic cancer. Using nanoparticles as carrier for immunotherapeutic agents for tumor-targeted delivery can attain the benefits associated with the local therapy with the convenience of systemic injection.

Among many nanoparticles being studied, glycol chitosan nanoparticle (CNP) was selected for this study to target tumor and TME. CNP is formulated from a natural polymer, chitosan, which is the essential structural element in the exoskeleton of crustaceans. Hydrophobically modified glycol chitosan polymer self-assembles into a nanoparticle in hydrophilic environment and is biocompatible and biodegradable **[24]**. When systemically administered, CNP selectively accumulates in tumor by the enhanced permeability and retention effect. Its comparatively low off-site accumulation, such as in the reticuloendothelial system, reduces the chance of side effects and enhances the tumor-targeting ability. Overall, CNP is an exceptional carrier for delivering various diagnostic, therapeutic, and/or imaging agents to tumor and TME **[25-28]**.

In this study, CD40-binding peptide that agonistically binds to CD40 receptor was chemically conjugated to CNP for tumor-targeted delivery. CD40-binding peptide used in this study mimics a portion of CD154, a CD40 ligand, on the helper T cells in human **[29]**. The main focus of this study is on the activation or re-education of macrophages in the tumor region towards anti-tumor immunity by inducing localized CD40 binding through systemically administered CD40p-CNP. Additionally, direct initiation of tumor cell death upon CD40 binding that can cause the inhibition of tumor growth *in vivo* and the production of tumor-associated antigens for priming antigen-presenting cells was identified **(Figure 1)**.

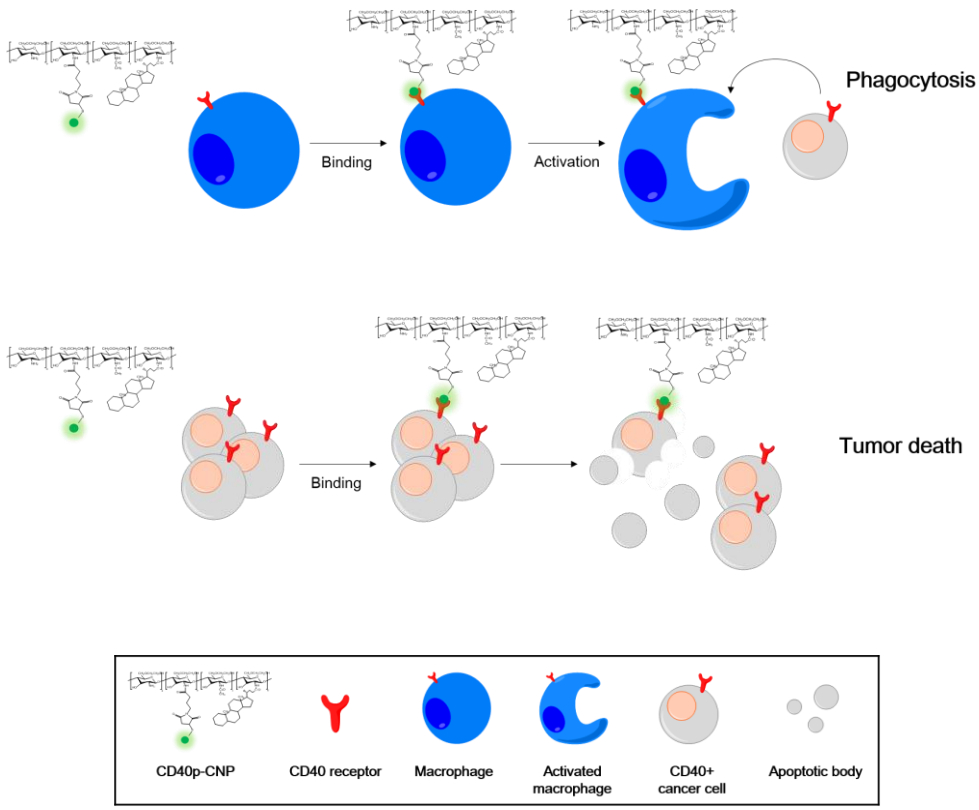

Figure 1. Schematic illustration of CD40 binding mechanisms in tumor microenvironment

2. Materials and Methods

2.1 Materials

Glycol chitosan (Mw = 2.5 × 10^5 Da; degree of deacetylation = 82.7 %), 5β-cholanic acid, N-hydroxysuccinimide (NHS), N-Methylomorpholine (NMM), 1-ethyl-3(-3-dimethylaminoprophyl)-carbodiimide hydrocholoride (EDC), and 4-(Dimethylamino)phyridine (DMAP) were purchased from Sigma-Aldrich Co. (St. Louis, MO, USA). Dimethyl sulfoxide (DMSO) was purchased from Daejung Chemicals & Metals Co., Ltd. (Gyeonggi, Republic of Korea). Methanol was purchased from Merck (Darmstadt, Germany). Sodium chloride (NaCl) was purchased from Duchefa Biochemie (Amsterdam, Netherlands). Cellulose membrane (MWCO = 12 – 14 kDa) was purchased from Spectrum Laboratories, Inc. (Rancho Dominquez, CA, USA). N-(γ-maleimidobutyryloxy)sulfosuccinimide ester (Sulfo-GMBS) was purchased from Thermo Fisher Scientific (Waltham, MA, USA). CD40-binding peptide (CD40p, Mw = 1,778 Da, Sequence: HGWYFYTKPLHLGGC) was purchased from Peptron (Daejeon, Republic of Korea). Near-infrared fluorescence (NIRF) dye, Flamma® 675 NHS ester (equivalent of Cy5.5, excitation and emission wavelengths of 675 nm and 691 nm, respectively), was purchased from BioActs (Incheon, Republic of Korea). D_2O and DMSO-*d6* were purchased from Cambridge Isotope Laboratories (USA).

THP-1 (Human acute leukemic monocyte) cell line was purchased from Korean Cell Line Bank (Seoul, Republic of Korea). U87 (Human glioblastoma), and B16F10 (Mouse melanoma) cell lines were purchased from American Type Culture Collection (ATCC; Rochkville, MD, USA). For cell culture, RPMI-1640, trypsin-EDTA, fetal bovine serum (FBS), 100x antibiotic antimycotic solution (AA) and Dulbecco's phosphate-buffered saline (DPBS) were purchased from

Welgene, Inc. (Gyeongsan, Republic of Korea). HEPES (4-(2-hydroxyethyl)-1-piperazineethanesulfonic acid) was purchased from Thermo Fisher Scientific (Waltham, MA, USA). Lipopolysaccharide (LPS) and Phorbol 12-myristate 13-acetate (PMA) were purchased from Sigma-Aldrich Co. (St. Louis, MO, USA). Cell counting kit-8 (CCK-8) was purchased from Dojindo Molecular Technologies, Inc. (Rockville, MD, USA). 5-week-old male C57BL/6 mice were purchased from Orient (Gyeonggi-do, Republic of Korea).

2.2 Synthesis of glycol chitosan nanoparticles

Hydrophobically modified glycol chitosan nanoparticles (CNP) were synthesized from glycol chitosan polymer (GC), as previously reported **[25-26]**. 1 g of GC was dissolved in 320 mL of distilled water and filtered by Millpore Millex-SV 5.00 μm syringe driven filter unit. Filtered GC solution was freeze-dried for 3 days. In order to hydrophobically modify GC for nanoparticle formation, 500 mg of filtered GC (2 μmol) was dissolved in 62 mL of distilled water, and 150 mg of 5β-cholanic acid (CA; 416 μmol) was dissolved in 114 mL of methanol. Then, the GC solution was mixed with 120 mg of EDC/ 62 mL of methanol, and the CA solution was mixed with 72 mg of NHS/ 10 mL of methanol for 30 min. GC/ EDC mixture was added to CA/ NHS mixture in drops and stirred for 24 h at room temperature for carboxyl-to-amine crosslinking. Following the conjugation, the solution was dialyzed against methanol/ distilled water mixture with gradual increase of water (4:1, 3:1, and 1:1, v/v) for 3 days, and against distilled water for 3 days using a cellulose membrane (MWCO = 12 – 14 kDa). Subsequently, the solution was lyophilized for 3 days and stored at –20 ℃.

2.3 Conjugation of CD40-binding peptide to CNP

To conjugate CD40p to CNP, sulfo-GMBS was used as an amine-to-sulfhydryl crosslinker. 18.6 mg of CNP (10.4 μmol) was dissolved in 600 μL DMSO and added to 9 mL PBS-EDTA (pH 7.4). Simultaneously, 1 mg sulfo-GMBS (2.6 μmol) was dissolved in PBS-EDTA (pH 7.4), and added to the CNP mixture. The mixture was stirred at room temperature for 2h in the dark to achieve maleimide activated CNP. 7.18 mg of CD40p (4.0 μmol) was dissolved in 1 mL distilled water and added to the CNP mixture. It was then stirred at room temperature for 6h in the dark. This reaction induced the binding of maleimide of CNP and cystein of CD40p. The resulting product was dialyzed against distilled water for 4 days and lyophilized for 3 days. The lyophilized CD40p-CNP was stored at –20 ℃.

2.4 Labeling of peptide and nanoparticles with Cy5.5

For imaging purpose, CD40p, CNP, and CD40-CNP were labeled with a NIRF dye, Cy5.5-NHS. To begin with, CD40p was conjugated with Cy5.5-NHS. 10 mg of CD40p (5.6 μmol) and 6.3 mg of Cy5.5-NHS (5.6 μmol) were dissolved in 300 μL of DMSO each. The Cy5.5-NHS mixture was slowly added to the CD40p mixture, and 70 μL of N-Methylomorpholine (NMM) and 0.6 mg of 4-(Dimethylamino)phyridine (DMAP) were added to the whole mixture. The reaction took place at room temperature (RT) for 2 h in the dark. Then, the mixture was purified by High performance liquid chromatography (HPLC) to remove unreacted materials and was subsequently lyophilized. The resulting Cy5.5-CD40p was stored at – 20 ℃.

To prepare Cy5.5-CNP and CD40p-CNP-Cy5.5, CNP was first conjugated to Cy5.5-NHS. 220mg of CNP was dissolved in 80 mL of DMSO. 2 mg of Cy5.5-NHS (1.7 μmol) was also dissolved in 500 μL DMSO. The Cy5.5-NHS mixture was added to the CNP mixture in drops and the resulting mixture was stirred overnight at room temperature in the dark. Then, the mixture was dialyzed against 5 L of distilled water with 40 g NaCl for 1 day and against distilled water for the following 3 days using a cellulose membrane (MWCO 12-14 kDa). After dialysis, the product was lyophilized and stored at –20 ℃.

For further conjugation of CD40p to Cy5.5-CNP, 7.8 mg of Cy5.5-CNP was dissolved in 200 μL of DMSO and added to 4.8 mL 1mM PBS-EDTA (pH 7.4). 0.42 mg of sulfo-GMBS was dissolved in 100 μL of 1mM PBS-EDTA (pH 7.4) and immediately added to the Cy5.5-CNP mixture. The mixture was shaken at room temperature for 2 h in the dark. 3 mg of CD40p was dissolved in 500 μL of distilled water and added to 500 μL of 1 mM PBS-EDTA (pH 7.4). The CD40p

solution was then added to the Cy5.5-CNP-linker mixture and shaken at room temperature for 6 h in the dark. The resulting product was dialyzed against distilled water for 4 days, lyophilized, and stored at –20 ℃.

2.5 Characterization of nanoparticles

The size distributions and surface zeta potentials of the nanoparticles (CNP, CD40p-CNP, Cy5.5-CNP, and CD40p-CNP-Cy5.5) were analyzed by Dynamic Light Scattering Zetasizer Nano ZS90 (Malvern Instruments Ltd, Malvern, UK). 1 mg of nanoparticles were dispersed in 1 mL distilled water for the measurement of size and zeta potential. To observe the shape of the nanoparticles at the concentration of 1 mg/ mL in distilled water, transmission electron microscopy (TEM, CM30 electronmicroscope, Philips, CA) was employed. The samples for TEM observation were prepared by placing dispersed nanoparticles on a 200 mesh copper grid coated carbon (Electron Microscopy Sciences, PA, USA) for 3 min. Any excess was absorbed with filter paper, and 2 % (w/v) uranyl acetate was dropped on the grid for negative staining. The chemical conjugation of CD40p to CNP was determined by 600 MHz-1H NMR (DD2 600 MHz FT NMR, Agilent Technologies, USA). For the NMR analysis, 2 mg of the nanoparticles were dissolved in 500 μL of DMSO-D6 and 500 μL of D_2O was added.

To quantify the amount of CD40p in CD40p-CNP, the intrinsic fluorescence of tryptophan (excitation wavelength: 280 nm) in CD40p was measured by Biophotometer plus (Eppendorf, Hamburg, Germany) **[30]**. Standard curve was drawn using selected concentrations of CD40p (0 – 1,000 μg/ mL distilled water), and the absorbances of CNP and CD40p-CNP (1 mg/ mL distilled water) were measured. The absorbance value of CNP was subtracted from the absorbance value of CD40p-CNP, and the amount of CD40p was determined from the standard curve.

2.6 Cell culture

THP-1 (Human acute leukemic monocyte) with the passage numbers from 2 – 15 were cultured in RPMI 1640 medium supplemented with 10 % (v/v) of FBS, 1 % (v/v) of AA, and 10 mM HEPES. U87 cells (Human glioblastoma) and B16F10 cells (Mouse melanoma) were cultured in RPMI 1640 medium supplemented with 10 % (v/v) of FBS, 1 % (v/v) of AA. Depending on the type of experiment, U87 and B16F10 were also cultured in RPMI 1640 growth medium with 10 mM HEPES. The cells were incubated under humidified 5 % CO_2 atmosphere at 37 ℃. To differentiate THP-1 monocytes to macrophages, the cells were seeded at 2 x 10^5 cells/ mL growth medium with 50 ng/ mL PMA. The medium was changed to remove PMA after 24 h. Further incubation of 48 h without PMA induced change in morphology that indicates complete differentiation **[31, 32]**.

Differentiation of macrophage was confirmed by morphology and flow cytometry. THP-1 (2 × 10^5 cells / dish) and differentiated THP-1 (2 × 10^5 cells / dish) were blocked by 1 % BSA / DPBS on ice for 30 min. After blocking, 0.05μg Alexa Fluor® 488 Rat IgG2b, κ Isotype Ctrl antibody and Alexa Fluor® 488 anti-mouse/human CD11b antibody (Biolegend, CA, USA) that is the marker of macrophage was added into cell samples, and samples were incubated on ice for 1h in the dark. After incubation, cell samples were centrifuged at 4℃ (450 xg, 5 min) and washed with DPBS (pH7.4). Once again, cell samples were centrifuged at 4℃ (450 xg, 5 min). Cell samples were suspension with DPBS (pH 7.4), and the intensity of cell samples was measured by Flow cytometry (Merck Millipore corporation, Darmstadt, Germany).

2.7 *In vitro* uptake of nanoparticles by differentiated macrophages

To observe the effect of CD40p on cellular uptake, THP-1 (4×10^5 cells / dish) were plated on 35 mm glass bottom dishes (SPL Life Sciences, Gyeonggi-do, Republic of Korea) and differentiated with PMA. The cells were then incubated with Cy5.5-CD40p (2.5 μg/ mL), Cy5.5-CNP (50 μg/ mL), or CD40p-CNP-Cy5.5 (75 μg/ mL) for 0 h, 0.5 h, 1 h, 3 h, 6 h, 9 h, 12 h, 18 h, and 24 h. The concentrations were adjusted for all samples to match the fluorescence intensity of Cy5.5. After the incubation, the cells were washed with DPBS (pH 7.4) and fixed with 4 % paraformaldehyde. The nuclei were stained with DAPI. Confocal images were obtained by Confocal laser microscope (Leica TCS SP8, Leica Microsystems GmbH, Germany) with 405 diode (405 nm), Ar (458, 488, 514 nm), and He-Ne (633 nm) laser.

2.8 *In vitro* toxicity

The cytotoxicity of the nanoparticles or the peptide on differentiated THP-1, B16F10, and U87 were evaluated with CCK-8 assay. B16F10, and U87 were seeded at 2.5 × 10^3 cells/ 100 μL growth medium/ well on a 96-well plate and incubated for 24 h. THP-1 were seeded at 2×10^4 cells/100 μL growth medium/ well on a 96 well plate and 50 ng/ mL PMA was added to each well. After 24 h, the medium was changed to remove PMA and further 48 h incubation was followed for complete differentiation. The cells were then treated with various concentrations of CD40-binding peptide, CNP, or CD40p-CNP (0, 0.25, 2.5, 10, 25, 50, 100 μM) for 24 h. After changing the media at 24 h, CCK-8 solution (10 μL/ well) was added and the cells were incubated for 3 h. The absorbance of wells was read at 450 nm with a microplate reader (Molecular Devices, CA, USA). Cell viability was calculated as the percentage of the viable cells in treatment group to the viable cells in untreated control group.

2.9 *In vitro* phagocytosis assay

Prior to the phagocytosis assay, THP-1 monocytes were differentiated to macrophages for 72 h. The differentiated THP-1 were further activated with the addition of CD40p (0.25, 2.5, 25 μM), CD40p-CNP (1.25, 12.5, 125 μM), CNP (1, 10, 100 μM) (0.25, 2.5, 25 μM of CD40p for CD40p and CD40p-CNP, and same molar concentration of CNP as used in CD40p-CNP), or LPS (0.036 μM) for 24 h. The level of activation was determined by morphology, western blot, and phagocytosis assay. After the activation, U87 cancer cells were added to the macrophages at a ratio of 1:5 (number of macrophages to cancer cells). The cell mixtures were incubated at 37 ℃ for 2 h and washed in ice-cold PBS (pH 10.0). The macrophages undergoing phagocytosis were observed by optical microscope (Olympus CK40, Tokyo, Japan). The number of macrophages undergoing phagocytosis was counted and recorded.

For flow cytometry analysis, differentiated THP-1 were treated with PBS, CD40p (0.25, 2.5, 25 μM), CD40p-CNP (1.25, 12.5, 125 μM), CNP (1, 10, 100 μM), or LPS (0.036 μM) for 24 h. After treatment, the differentiated THP-1 cells were stained by adding 1 μM of CellTracker™ Deep Red and U87 cells were stained by adding 0.5 μM of CellTracker™ Green for 30 min. Then, the stained U87 were added directly to the stained differentiated THP-1 cells and co-cultured for 2 h **[33]**.

2.10 *In vivo* and *ex vivo* imaging in tumor-bearing mice

All experiments using live animals were carried out in compliance with the relevant laws and institutional guidelines of Korea Institute of Science and Technology (KIST). To monitor *in vivo* accumulation of Cy5.5-CD40p, Cy5.5-CNP and CD40p-CNP-Cy5.5 in tumors, 5-week-old C57BL/6 mice were prepared (n= 3/ group, average weight: 19 g). The mice were subcutaneously inoculated with B16F10 (1×10^6 cells/ 80 μL DPBS/ mouse) into the left flank. When the size of the tumors reached 0.5-1 cm per axis, the mice were used for imaging. The concentrations of Cy5.5-CD40p, Cy5.5-CNP, and CD40p-CNP-Cy5.5 dispersed in DPBS were adjusted to have matched fluorescence intensity. Cy5.5-CD40p, Cy5.5-CNP, and CD40p-CNP-Cy5.5 were injected intravenously through the tail vein into the tumor-bearing mice. The accumulations of the injected peptide or nanoparticles in mouse tumors were monitored at 1, 6, 12, 24, 48 h post-injection by using an eXplore Optix system (ART Advanced Research Technologies Inc., Montreal, Canada) with 670 nm-pulsed laser diode. For the complementary *ex vivo* analysis, mice were sacrificed after 48 h of imaging. The tumors were dissected and the fluorescence intensities were quantified with IVIS Lumina Series Ⅲ (PerkinElmer, MA, USA).

2.11 Evaluation of *in vivo* tumor growth inhibition

To evaluate the effect of CD40p-CNP on the inhibition of tumor growth, 5-week-old C57BL/6 mice were subcutaneously inoculated with B16F10 (1×10^6 cells / 80 μL DPBS/ mouse) into the left flank. When the size of the tumors reached 40 – 100 mm^3, the therapy was initiated. The mice were divided into three groups (n= 3/ group, average weight: 19 g): the first control group treated with intravenous injection of PBS, the second group treated with intratumoral injection of CD40p (4 μg/ mouse), and the third group treated with intravenous injection of CD40p-CNP (40 μg/ mouse). The injections were performed every two or three days for 16 days or until the volume of the untreated control tumors reached 2500 mm^3. The minor and the major axes of the tumors were measured with a digital caliper. Tumor volume was computed by using the following formula: (The volume of tumor) = (Major axis) × $(\text{Minor axis})^2 \times 0.52$. The mice were euthanized when the volume of the tumors reached 2000 – 2500 mm^3.

2.12 Western blot analysis

The activation of macrophage *in vitro* and *in vivo* after treatment were evaluated by performing Western blot. For *in vitro* analyses, differentiated THP-1 were either mono-cultured or indirectly co-cultured with U87. Indirect co-culture of differentiated THP-1 with U87 was performed using 24 mm Transwell® with 0.4 μm pore (Corning, New York, USA) **[34]**. PBS, CD40p (0.25, 2.5, 25 μM), CD40p-CNP (1.25, 12.5, 125 μM), CNP (1, 10, 100 μM), or LPS (0.036 μM) were added to the differentiated THP-1 and incubated for 24 h. The media were removed after 24 h and the cells were washed with ice-cold DPBS (pH 7.4). Ice-cold RIPA buffer with protease inhibitor cocktail (Invitrogen, CA, USA) was added to the cells and the cells were incubated on ice for 30 min. The cells were scraped off the dishes and collected in 1.5 mL microcentrifuge tubes. The lysates were centrifuged at 4 ℃ (12,000 rpm, 10 min). For *in vivo* analysis, the excised tumors from the three groups (control, CD40p (I.T.), and CD40p-CNP (I.V.) were homogenized using a Wise Mix homogenizer (DH science, Incheon, Republic of Korea) after adding RIPA lysis buffer with protease inhibitor cocktail. The homogenized tumor lysates were centrifuged twice at 4 ℃ (12,000 rpm, 10 min) to collect the supernatants. Protein concentrations were determined by BCA protein assay (Thermo Fisher Scientific, MA, USA). SDS sample buffer was added to the lysates containing 35 μg protein, and the samples were boiled at 95 ℃ for 5 min. 12 % (w/v) polyacrylamide gel was used for SDS-PAGE. After transfer, the membranes were blocked with 5 % skim milk in Tris buffered saline with 0.05 % Tween-20 (TBST) for 45 min. Primary antibodies of phospho-p38 (Cell Signaling Technology, MA, USA), p-38 (Cell Signaling Technology, MA, USA), IL-12 (LifeSpan BioSciences, Inc., WA, USA) and β-actin (Abcam, Cambridge, UK)

were added to the blocking solution and incubated at 4 ℃ overnight **[35]**. Subsequently, the membranes were washed three times with TBST and incubated with horseradish peroxidase (HRP)-conjugated secondary antibodies in blocking solution for 1 h. After the secondary antibody incubation, the membranes were washed three times, and developed using an ECL substrate (Thermo Fisher Scientific, MA, USA). The chemiluminescence signals were detected by Image Reader LAS-3000 (Fujifilm, Tokyo, Japan). Quantification of western blot bands were performed by using Image J software.

2.13 Histological evaluation

The tumors from the three treatment groups (Untreated control, CD40p (I.T.), and CD40p-CNP (I.V.)) were fixed in 4% formaldehyde solution. The fixed tumors were dehydrated and embedded in paraffin, and sectioned to the thickness of 6 μm for histological evaluation.

Prior to staining, the tissue slides were deparaffinized and rehydrated. The slides were placed in a 60 ℃ oven for 15 min to melt the paraffin and washed twice with xylene to remove the paraffin. The samples were rehydrated by graded washes of ethanol in water (100 % to 70 %), ending in washes with distilled water. For the immunohistochemical staining of CD68, the endogenous peroxidase activities were quenched with 3 % hydrogen peroxide solution and antigens were retrieved by boiling the slides in sodium citrate buffer (pH 6.0) for 10 min. After cooled to room temperature, the slides were washed with DPBS containing 0.05 % Tween-20 (PBST), and anti-CD68 primary antibody (1:200 in DPBS; Abcam, Cambridge, UK) were applied to the slides. The slides were incubated overnight in a wet chamber at 4 ℃. The next day, the tissue slides were washed with PBST and incubated with HRP-conjugated secondary antibody (Agilent Technologies, CA, USA) for 40 min in a wet chamber. After PBST wash, DAB substrate solution (Agilent Technologies, CA, USA) was added to the slides and incubated in a wet chamber for 3-10 min until the color developed. Then the tissue slides were washed with distilled water and stained with hematoxylin (Sigma-Aldrich Co., MO, USA). The stained slides were washed thoroughly with distilled water and dehydrated by immersing the slides in a series of ethanol (95 % to 100 %) and xylene. The slides were mounted with Permount™ Mounting Medium (Fisher Scientific, MA, USA).

For hematoxylin and eosin staining, the tissue slides were removed of

paraffin and rehydrated under the same conditions as IHC staining. The sections were then rinsed with distilled water and immersed in hematoxylin for 8 min to stain the nuclei. Following rinsing in running tap water, the tissues were differentiated with 1 % acid alcohol and again rinsed in running tap water. Subsequently, 0.2 % ammonia water was used to blue up the slides and the slides were repeatedly rinsed in tap water. Counterstaining was achieved by immersing the slides in eosin Y solution (Sigma-Aldrich Co., MO, USA) for 2 min. The slides were dehydrated through a series of ethanol (95 % to 100 %), cleared in xylene, and mounted with Permount™ Mounting Medium.

3. Results and discussion

3.1 Formulation and characterization of CD40p-CNP

According to a previous study that analyzed tumor-targeting efficiency of five types of nanoparticles, prolonged circulation in the bloodstream and evasion from the reticuloendothelial system enhanced the tumor-targeted delivery of nanoparticles **[36]**. In this study, CNP demonstrated the longest circulation, the lowest reticuloendothelial clearance, and the highest tumor accumulation when compared to polystyrene nanoparticle, TiO_2-encapsulated carboxymethyl dextran nanoparticle, hyaluronic acid nanoparticle, and dextran sulfate nanoparticle. Based on the result, CNP was selected as a carrier to deliver CD40p to tumor and TME.

Prior to CD40p conjugation, CNP was prepared. The amine groups of linear polymer of glycol chitosan formed amide bonds with hydrophobic 5β-cholanic acid in the presence of EDC and NHS to construct a self-assembled nanoparticle. Then, CD40p-CNP was synthesized in two steps. The leftover amine groups of CNP that had not participated in 5β-cholanic acid conjugation were reacted with sulfo-NHS ester of sulfo-GMBS crosslinker to form maleimide activated CNP. It was then reacted with the sulfhydryl group of cysteine in CD40p (**Figure 2**). In addition, for *in vitro* and *in vivo* imaging purposes, Cy5.5-NHS (Ex: 675 nm, Em: 694 nm) was chemically attached to CD40p and CNP. Cy5.5-NHS-labeled CNP was used to formulate CD40p-CNP-Cy5.5. For Cy5.5-CD40p conjugation, the peaks of CD40p and Cy5.5-NHS were identified by high-performance liquid chromatography (HPLC) before the reaction. The fluorescence intensity peak of CD40p was non-existent, but Cy5.5-NHS was detected at 16.582 min. After the conjugation, the fluorescence intensity peak was shifted for Cy5.5-CD40p to 17.578 min to indicate

successful conjugation (**Figure 3**). The syntheses were also confirmed by NMR analysis. When CD40p-CNP was compared to CNP, peaks of benzene and imidazole protons in CD40p were observed at 6-8 ppm after successful conjugation (**Figure 4**).

Physicochemical properties of the nanoparticles were determined by dynamic light scattering (DLS) for particle size and surface charge, and transmission electron microscopy (TEM) for overall shape after the conjugation (**Figure 5**). When compared to CNP and Cy5.5-CNP, which had mean diameters of 266.39 ± 0.71 nm and 284.65 ± 4 nm, respectively, the sizes of CD40p-CNP and CD40p-CNP-Cy5.5 increased to 290.46 ± 3.81 nm and 353.76 ± 12.08 nm, respectively. TEM images of the nanoparticles showed a spherical shape. In addition, the surface charge increased for CD40p-CNP and CD40p-CNP-Cy5.5 (26.4 ± 2.69 mV and 22.6 ± 2.78 mV) than CNP (17.3 ± 0.32 mV) and Cy5.5-CNP (16.7 ± 0.44 mV), due to the charge of some amino acids of CD40p. The increase in size and zeta potential also confirmed the successful synthesis of CD40-CNP from CNP.

Intrinsic fluorescence of tryptophan in CD40p was used to monitor the loading efficiency by a biophotometer. The absorbances were read at 280 nm. The weight percentages of CD40p in CD40p-CNP and in CD40p-CNP-Cy5.5 were determined to be 22.29 ± 3.52 % and 21.17 ± 1.02 %, respectively. For all following experiments, the weight percentage of CD40p was approximated to be 20 %. (**Table 1**)

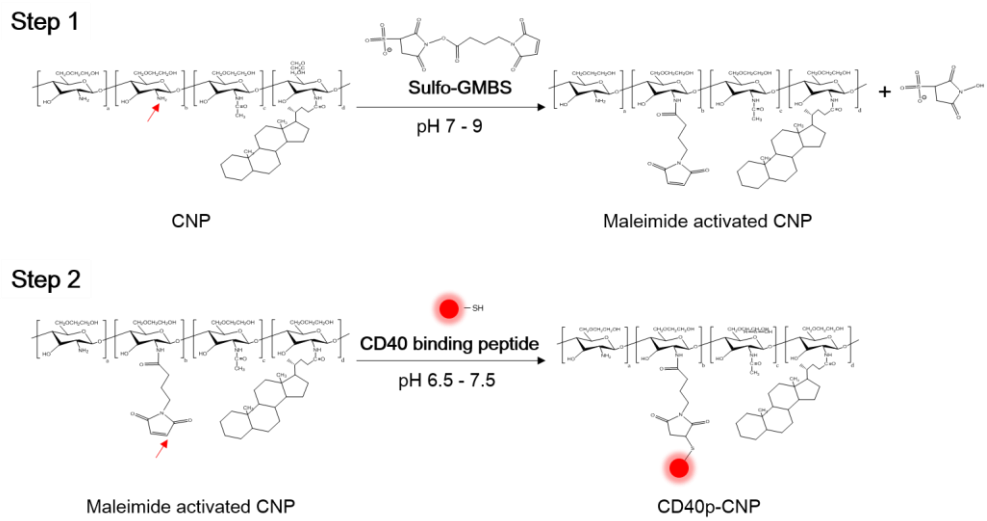

Figure 2. Conjugation of CD40-binding peptide to glycol chitosan nanoparticle (CNP)

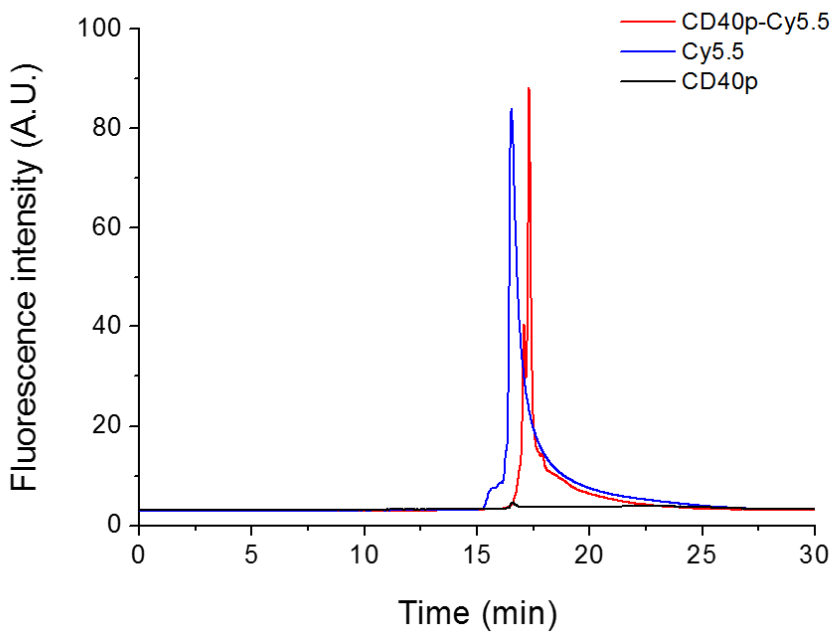

Figure 3. HPLC profiles of CD40p (Black), Cy5.5 (Blue, 16.582 min) and Cy5.5-CD40p (Red, 17.578 min).

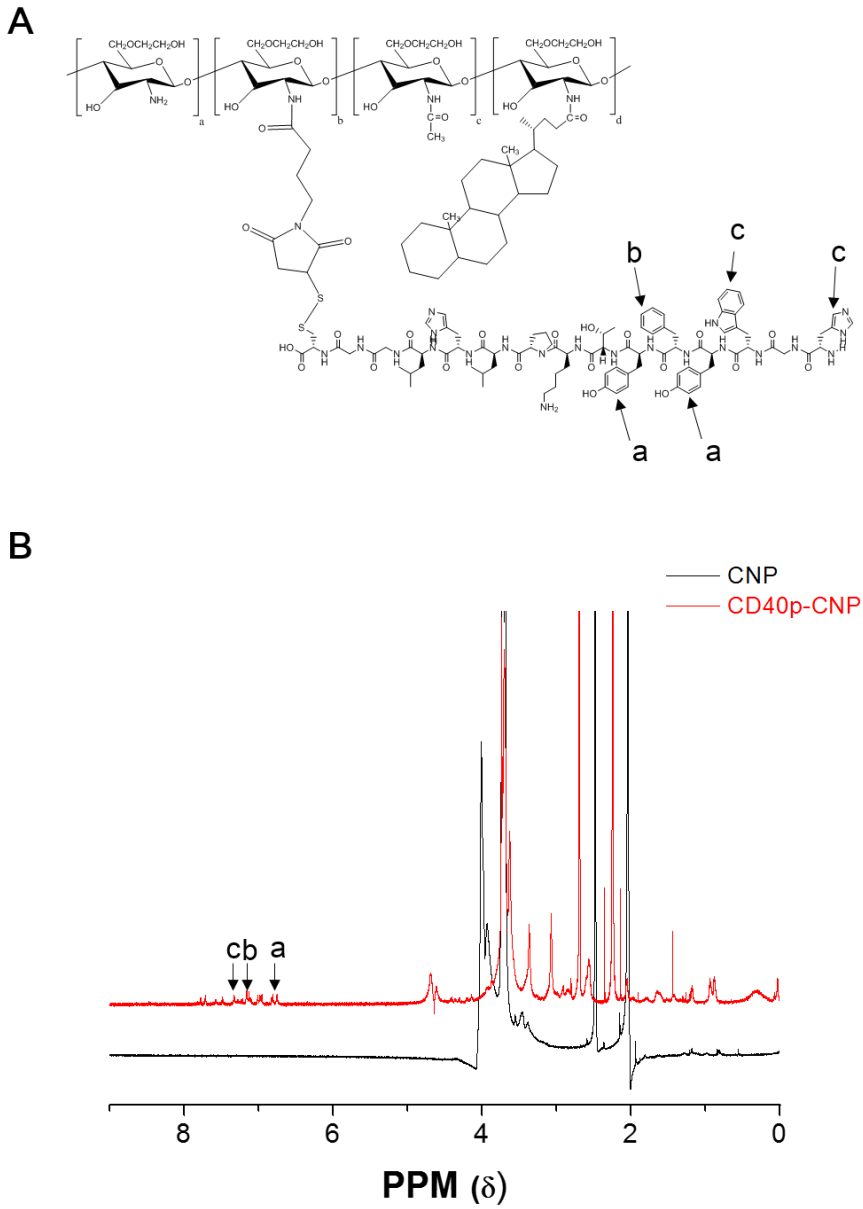

Figure 4. Identification of conjugation by 600 mHz ^{1}H NMR.

(A) Chemical structure of CD40p-CNP. (B) NMR analyses of CNP (Black) and CD40p-CNP (Red).

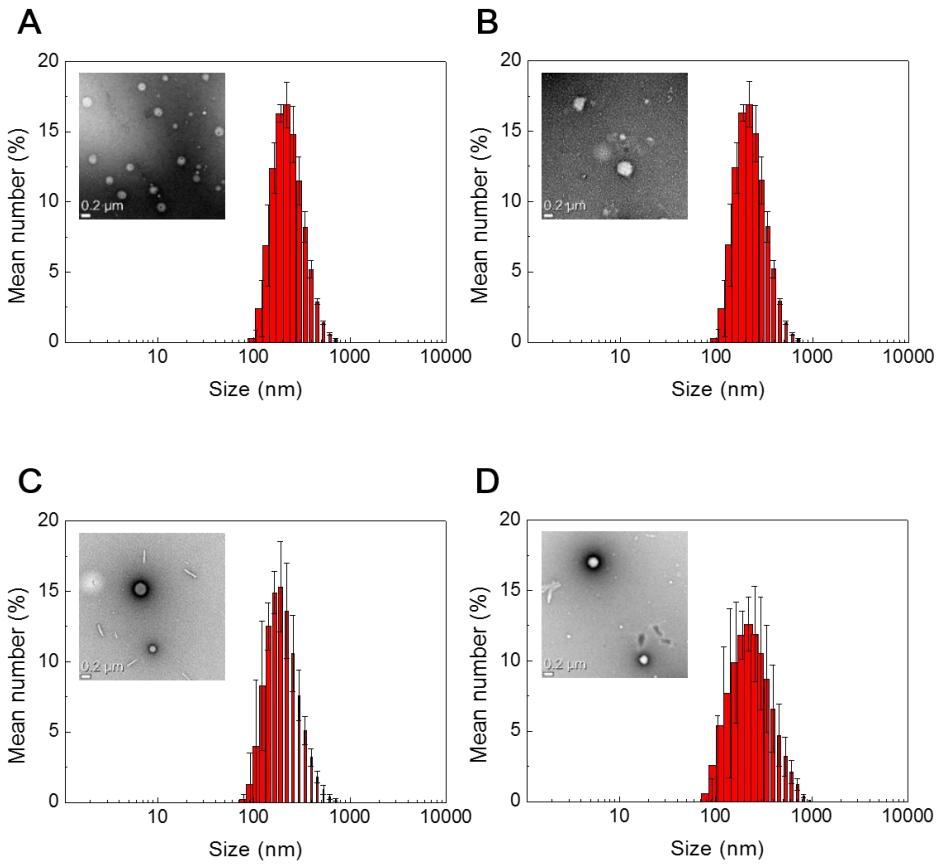

Figure 5. Characterization of nanoparticles by DLS and TEM. Size analyses and transmission electronic microscopic images of (A) CNP, (B) CD40p-CNP, (C) Cy5.5-CNP, and (D) CD40p-CNP-Cy5.5.

	Diameter (nm)[a]	Zeta potential (mV)[b]	PDI	CD40p (% wt)[c]
CNP	266.39±0.71	17.3±0.32	0.204	
Cy5.5-CNP	284.65±4	16.7±0.44	0.230	
CD40p-CNP	290.46±3.81	26.4±2.69	0.215	22.29±3.52 (125.34±19.78 nmol)
CD40p-CNP-Cy5.5	353.76±12.08	22.6±2.78	0.246	21.17±1.02 (119.05±5.71 nmol)

[a] Mean diameter measured by Dynamic Light Scattering (DLS)

[b] Zeta potential measured by Zeta sizer

[c] % CD40p determined by measuring absorbance using a biophotometer

Table 1. Size and surface charge of the nanoparticles and quantification of CD40-binding peptide in CD40-binding peptide-conjugated CNP. Weight percentages of CD40-binding peptide in conjugated nanoparticles were measured by biophotometry technique employing the intrinsic fluorescence of tryptophan in CD40p.

3.2 Cellular uptake of CD40p-CNP by differentiated macrophages

To observe the effect of CD40p conjugation to CNP on the interaction with differentiated macrophages, Cy5.5-labeled CD40p-CNP, CNP, and CD40p were added to previously differentiated THP-1 macrophages (**Figure 6**). 18 h incubation with CNP resulted in nanoparticle uptake by macrophages. However, CD40p-CNP was observed to be inside the macrophages after 3 h. Because CD40p was taken up quickly by the macrophages, the internalization of CD40p-CNP was concluded to be due to the presence of CD40p on CNP. Cellular uptake of nanoparticles was reported to be governed by several different endocytosis mechanisms, such as micropinocytosis, clathrin-mediated endocytosis, caveolae-mediated endocytosis, and phagocytosis [**37, 38**]. Since the interaction between CD40 ligand and CD40 receptor on the surface of macrophages increases phagocytic activity of macrophages **[19]**, it seems reasonable to conclude that activation of the macrophages by CD40p-CNP through CD40 receptor-mediated pathway expedited the uptake of the nanoparticle by differentiated THP-1 macrophages.

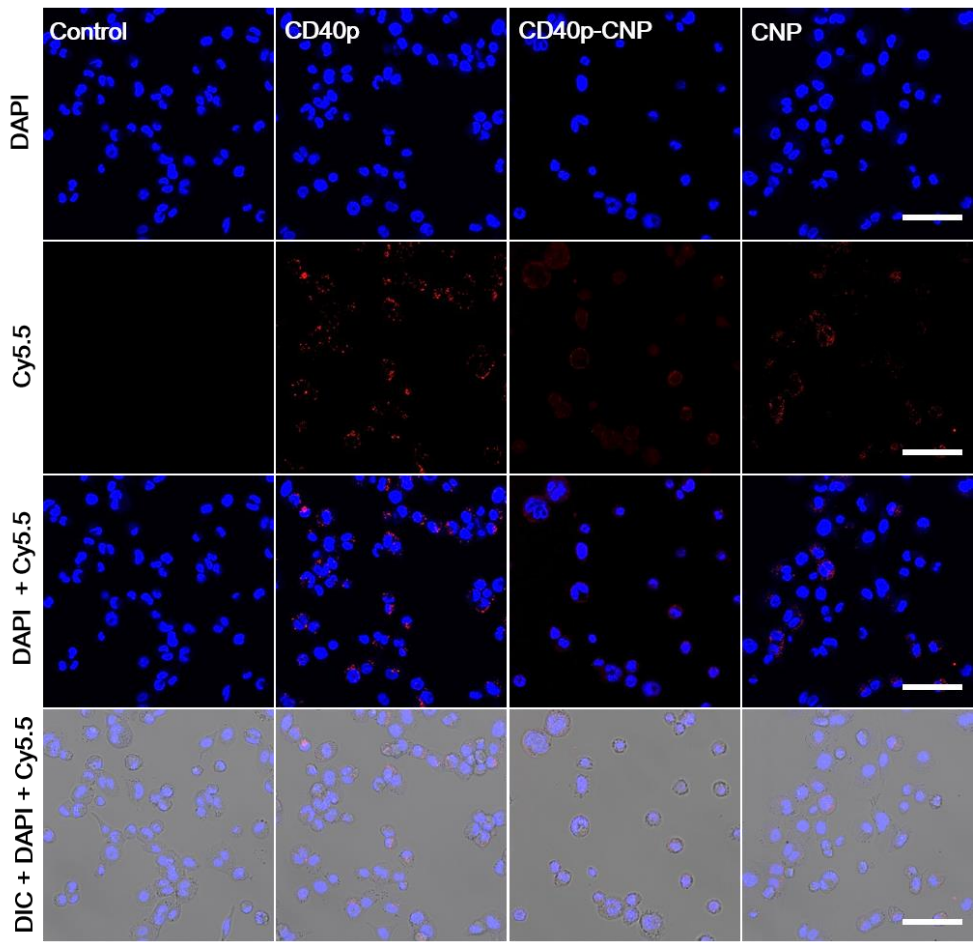

Figure 6. Cellular uptake images of peptides and nanoparticles by differentiated THP-1. The nuclei were stained with DAPI (blue) and CD40p, CD40p-CNP and CNP were shown in red. Durations and concentrations of treatments were as follows: CD40p (30 min, 2.5 μg/ mL), CD40p-CNP (3 h, 75 μg/ mL), and CNP (18 h, 50 μg/ mL). Scale bar represents 50 μm.

3.3 *In vitro* cytotoxicity analysis of CD40p-CNP

Next, we examined whether the receptor binding of CD40 induced death of cancer cells *in vitro*. Various concentrations of CD40p, CD40p-CNP, and CNP were added to B16F10 mouse melanoma cells, U87 human glioblastoma cells, and differentiated THP-1 macrophages. Cytotoxicity caused by the added peptide or nanoparticles was evaluated by CCK-8 assay after 24 h incubation. The viability of the cancer cells, B16F10, and U87 significantly decreased as the concentration of CD40p or CD40p-CNP increased (**Figure 7A & 7B**). CNP did not affect the viability of cancer cells. In comparison, the viability of differentiated macrophages was not affected by the addition of CD40p, CD40p-CNP, or CNP in all concentrations (**Figure 7C**). The results indicate that the binding of CD40 receptor on cancer cells by CD40p or CD40p-CNP lead to cell death, which in consequence can inhibit tumor growth *in vivo*. In addition, the death of tumor cells will produce tumor-associated antigens in the TME, recruiting and priming antigen-presenting cells for enhanced pro-inflammatory response against tumor. Meanwhile, CNP was demonstrated to be a versatile carrier with low cytotoxicity towards both cancer cells and macrophages even in high concentrations.

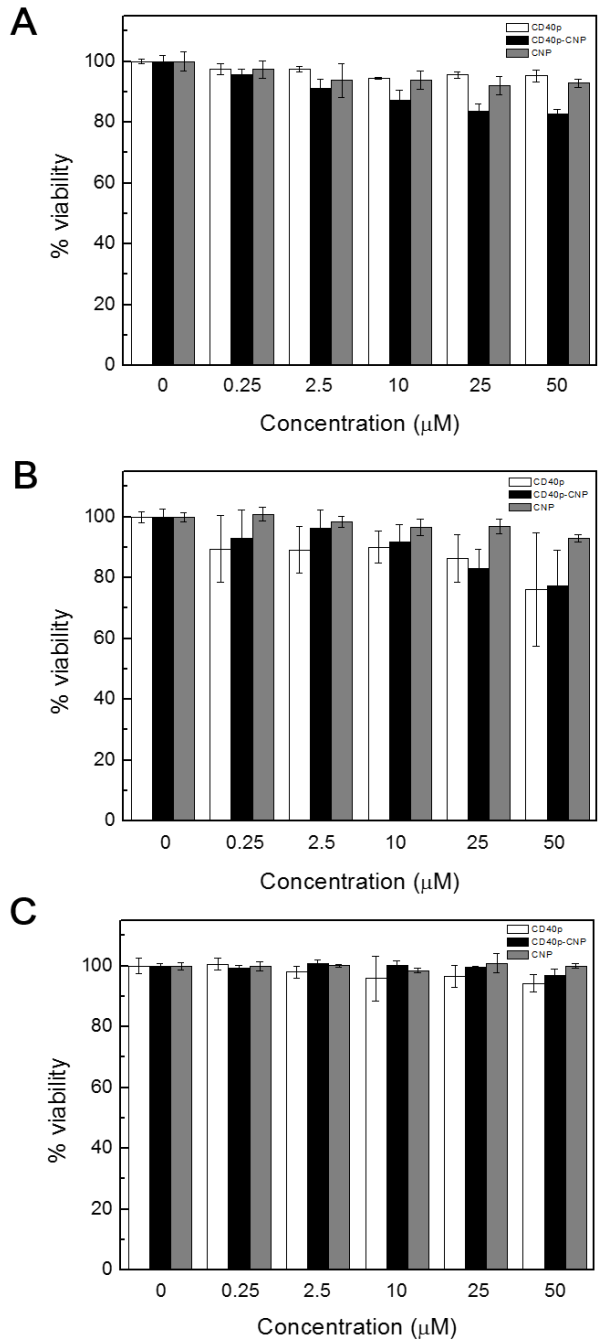

Figure 7. Cell viability assays in selected cell lines. (A) B16F10, (B) U87, and (C) differentiated THP-1.

3.4 Activation of macrophages by CD40p-CNP

Prior to observing activation of macrophages, differentiation of THP-1 monocytes into macrophages was confirmed by staining the differentiated cells with Alexa Fluor® 488 anti-CD11b (**Figure 8A**). CD11b is a known pan-macrophage marker that can differentiate macrophages from monocytes. Moreover, the differentiation was confirmed by observing the morphology of the cells that the monocytes were in suspension but the differentiated THP-1 adhered to the bottom of the culture vessel after the addition of 50 ng/ mL PMA to the cells (**Figure 8B**). In order to observe the effect of CD40 ligation on the activation of macrophages, three concentrations (0.25 μM, 2.5 μM, and 25 μM of CD40p and equivalent concentrations of CNP) of CD40p, CD40p-CNP, or CNP were added to differentiated THP-1 cells. LPS was used as a positive control for macrophage activation. The characteristic change in morphology following activation was more evident with the increased formation of lamellipodia in the two lower doses of CD40p or CD40p-CNP compared to the highest dose (**Figure 8B**). Western blot analysis also confirmed the enhanced macrophage activation by the two lower doses. The lower doses of CD40p resulted in more steep increase in the phosphorylation of p38 mitogen-activated protein kinase and the expression of interleukin-12, which are signaling molecules related to pro-inflammation and activation of macrophages. (**Figure 8C & 8D)**. A possible explanation of why the two lower doses of CD40p produced higher activation is that a significantly high concentration of CD40p might additionally induce stimulation of a different signaling pathway that regulates macrophage activation. The intrinsic nature of immune system tends to maintain homeostasis that intense signaling towards pro-inflammation is often counteracted by signals that provoke anti-inflammation.

Indeed, dual function signaling of CD40 has been reported in previous publications [**35, 39, 40**].

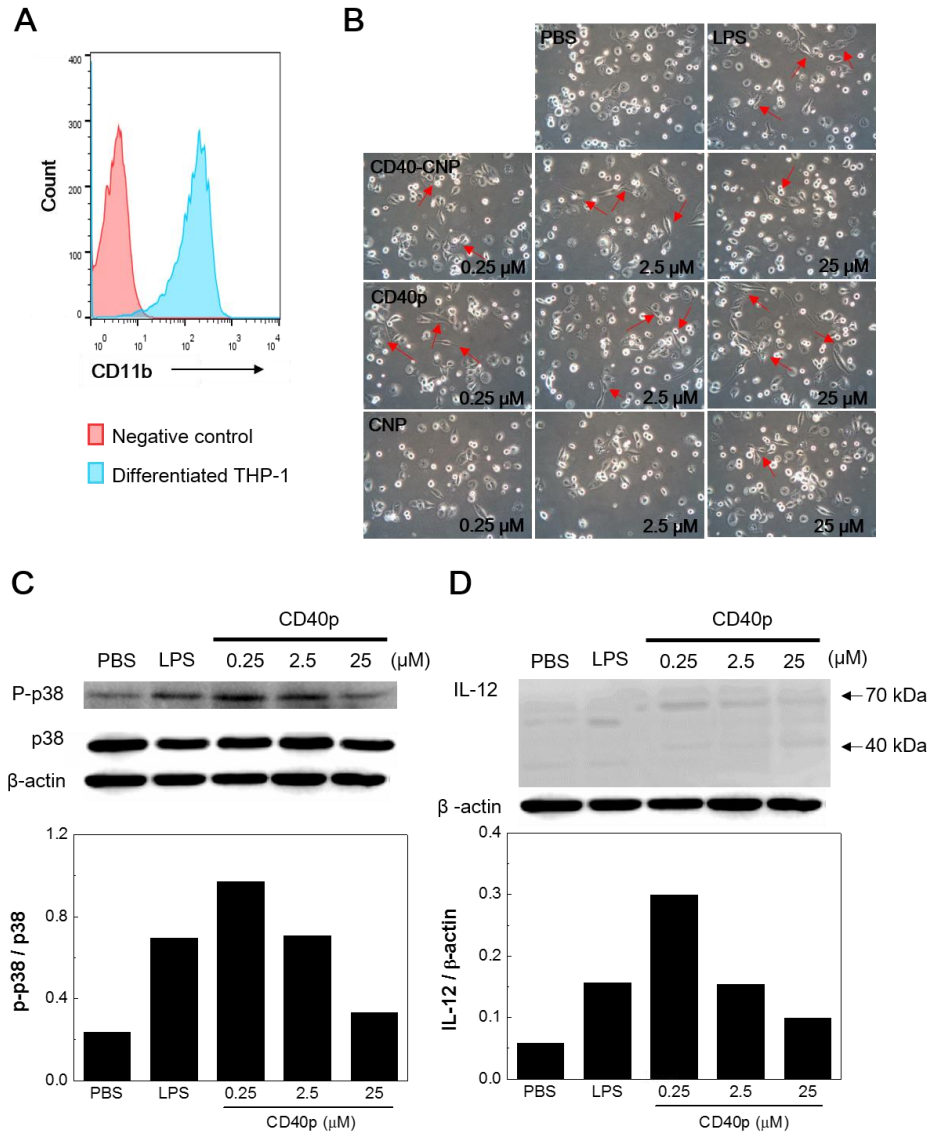

Figure 8. *In vitro* activation of differentiated THP-1. (A) Differentiation of THP-1 confirmed by FACS analysis. (B) Microscopic images of differentiated THP-1 after treatments. Red arrows indicate activated macrophages. Original magnification power was 400x. (C) Molecular changes of p-p38 / p38 and (D) Interluekin-12 (IL-12) / beta-actin in differentiated THP-1 following the treatments analyzed by Western blot.

3.5 Phagocytosis of cancer cells by macrophages upon activation by CD40p-CNP

After observing the role of CD40 binding in macrophage activation, phagocytosis assay was followed. Differentiated THP-1 were treated with three concentrations of CD40p, CD40p-CNP, or CNP, and incubated for 24 h. LPS was used as a positive control. Then, five times more number of U87 cancer cells in comparison to macrophages were added to the macrophage culture and co-cultured for 2 h. The 1:5 ratio of macrophages to cancer cells was used to mimic the cellular components of TME. After PBS wash, the cells were observed under a light microscope. Macrophages that underwent phagocytosis appeared larger in size, and debris of cancer cells in phagosomes were sometimes observed (**Figure 9A & 9B**). The incidents of phagocytosis were counted for each treatment. The macrophages treated with LPS, CD40p, or CD40p-CNP phagocytosed more number of cancer cells, whereas the macrophages treated with CNP did not show any significant change (**Figure 9C & 9D)**. Increased phosphorylation of p38 was observed after treatment with CD40p-CNP. (**Figure 9E**). The activation of the p38 pathway has been reported to play essential roles in the production of proinflammatory cytokines, such as IL-6, TNF-α, and IL-1β. Interestingly, the amount of phosphorylated p38 increased as the concentration of CD40p-CNP increased despite the results from the previous activation experiment and the following phagocytosis experiment that associated lower doses with more activation and more phagocytosis. A possible explanation is that in the downstream of p38 signaling there might be a regulatory pathway that becomes activated when the amount of phosphorylation of p38 exceeds a certain threshold. Maintaining homeostasis is important in many immunological pathways that such negative feedback mechanism is not uncommon. As mentioned before, for the phagocytosis

experiment, in accordance with the previous activation experiment the macrophages treated with the lower doses of CD40p and CD40p-CNP phagocytosed more than the ones treated with the highest dose. From the result, it can be concluded that the activation of macrophages through CD40 ligation by CD40p-CNP led to the increase in phagocytic activity of the macrophages.

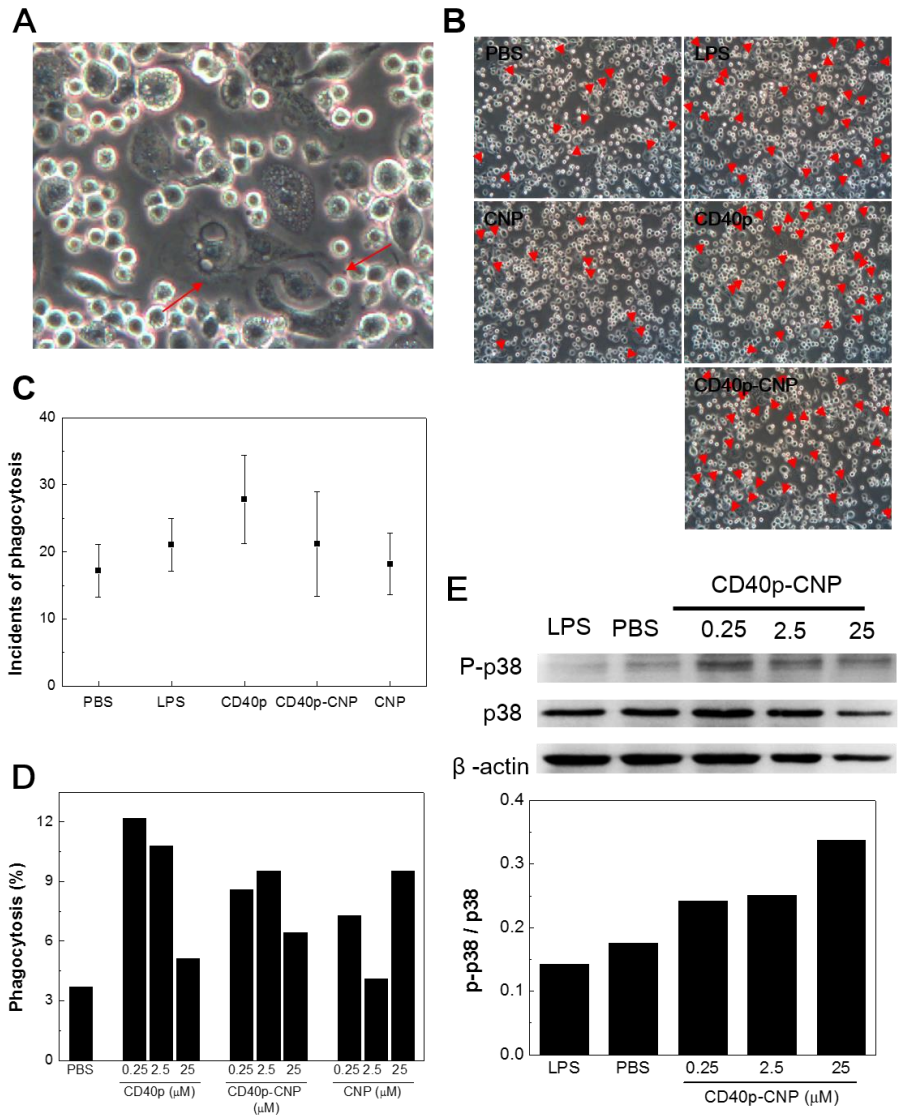

Figure 9. *In vitro* phagocytic activity of differentiated THP-1 after co-culture with U87 for 2 h. (A) Enlarged image of THP-1macrophages undergoing phagocytosis. (B) Total microscopic images of macrophages after co-culture. Red arrows indicate phagocytosis of cancer cells into macrophages. Original magnification power was 400x. (C) Number of macrophages undergoing phagocytosis manually counted from the microscopic images (n=5) and (D) analyzed by flow cytometry. (E) Molecular changes in differentiated THP-1 after treatments and co-culture analyzed by Western blot.

3.6 *In vivo* accumulation of CD40p-CNP in tumors

The *in vivo* accumulations of Cy5.5-labeled CNP, CD40p-CNP, and CD40p in tumor-bearing mice were monitored over time (**Figure 10A**). At 1 h post-administration, intense fluorescent signals were observed from the tumors of the mice that were injected with CNP or CD40p-CNP, indicating high accumulation of the nanoparticles in the tumors. In contrast, intravenously injected CD40p did not show significant accumulation in the tumors at all times. The fluorescent signals of CD40p-CNP from the tumors were the most intense between 12 h and 24 h post-injection, demonstrating significantly longer circulation of the nanoparticle when compared to CD40p. Accumulations of the injected nanoparticles and peptide in the tumors were confirmed by an *ex vivo* tumor analysis (**Figure 10B**). The fluorescent signals from the excised tumors were also quantified (**Figure 10C**). The fluorescence intensities from the tumors of CNP- or CD40p-CNP-injected mice were at least 1.3 times stronger than those from the tumors of CD40p-injected mice. The results show that conjugation of CD40p to CNP not only increases the amount of the accumulated peptide in the tumor region, but also considerably prolongs the duration of the CD40p accumulation in the tumor and TME.

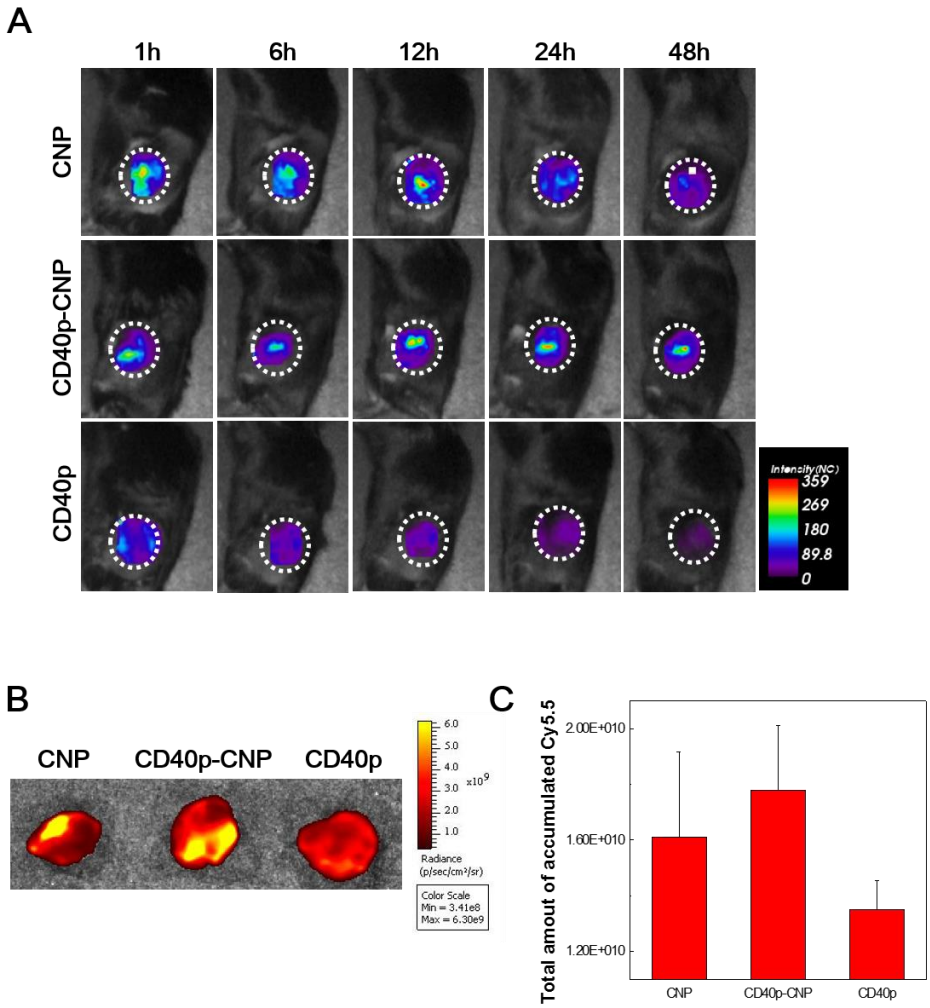

Figure 10. Time-dependent tumor accumulation of CNP, CD40p-CNP, and CD40p after intravenous injection. (A) *In vivo* tumor NIRF images of B16F10 tumor-bearing mice over time after nanoparticle/peptide injection. (B) *Ex vivo* NIRF images of tumors. (C) Total amount of fluorescence intensity in the tumors excised from the mice at 48 h after injection.

3.7 Inhibitory effect of CD40p-CNP on *in vivo* tumor growth

The effect of systemically administered CD40p-CNP on the tumor growth compared to the local administration of CD40p was evaluated using tumor-bearing C57BL/6 mice (**Figure 11**). The mice were divided into three groups: two experimental groups and one control group. For the experimental groups, each group was injected either intratumorally with CD40p or intravenously with CD40p-CNP. The control group was injected intravenously with PBS. The treatment doses and frequencies were determined based on the previous cytotoxicity result and the literatures **[41-43]**. The tumor volumes increased for all treatment and control groups, but the rate of the increase was the highest in the control group (**Figure 11B & 11C**). The rate of tumor growth in the control group was at least twice the rate of the other two treatment groups. The rates were comparable in the intratumoral injection group of CD40p and the intravenous injection group of CD40p-CNP. The molecular level analysis by Western blot confirmed the similarity between the intratumoral injection of CD40p and intravenous injection of CD40p-CNP that the increases in the phosphorylation of p38 were comparable in both groups. This outcome is noteworthy in the sense that the delivery of CD40p to tumor using CNP as a tumor-targeting carrier showed the similar result to the localized injections of CD40p. The result confirms that CNP is an efficient tumor-targeting carrier and the delivery of CD40p to tumor and TME induces successful inhibition of tumor growth *in vivo*.

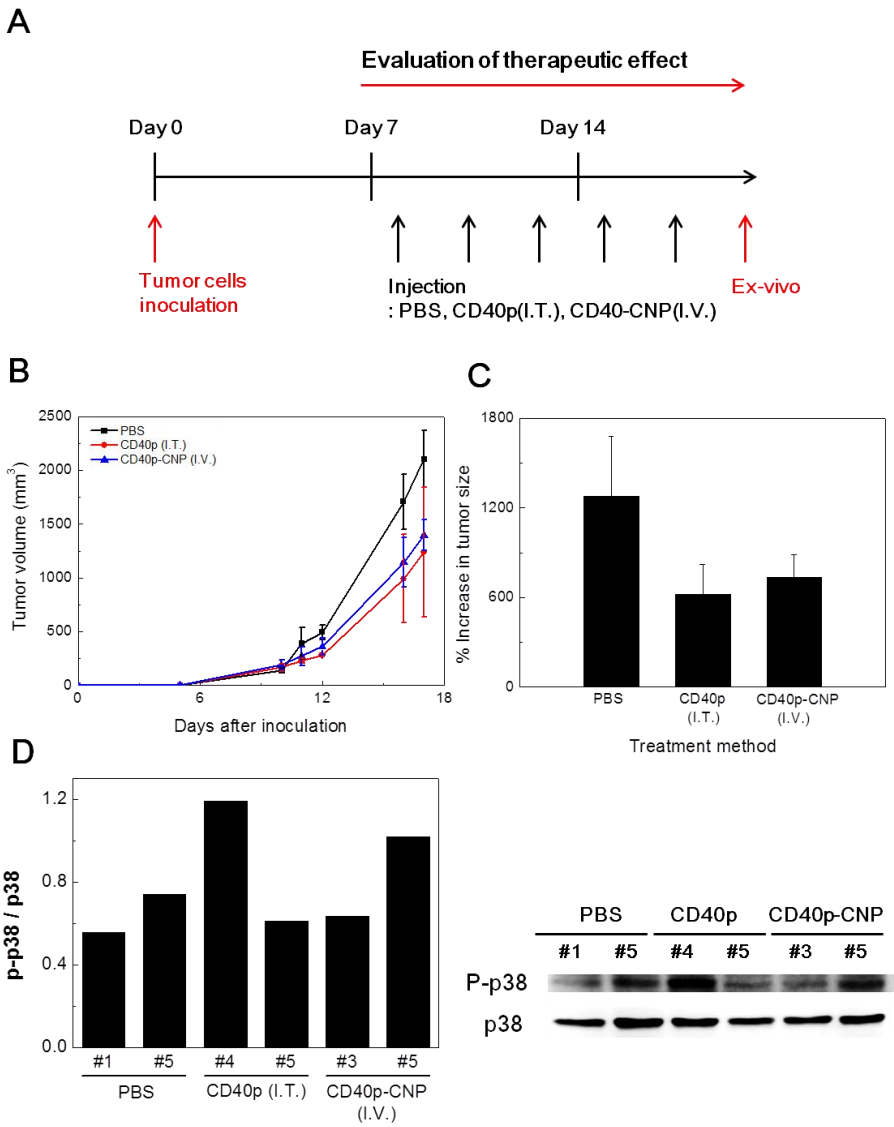

Figure 11. Effect of localized injection of CD40p or intravenous injection CD40p-CNP on the inhibition of tumor growth. (A) Timeline of the experiment (B) Measurements of the tumor volumes over time (C) Percentage of increase in tumor volumes after final treatments compared to the initial tumor volumes. (D) Molecular changes of p-p38 / p38 in tumor lysates from mouse tumor xenograft models after designed treatments

3.8 Histological analysis

Histological analysis was performed to identify changes in the cellular level following the treatments with CD40p (I.T.), CD40p-CNP (I.V.), or PBS. The excised tumor tissues were embedded in paraffin and sliced into thin sections. The tissue sections were deparaffinized and stained with hematoxylin and eosin for histological examination (**Figure 12A**). Necrotic deaths of tumor cells were sporadically observed in the tumors treated with CD40p or CD40p-CNP, confirming the cytotoxicity of CD40p towards tumor cells as shown in the previous *in vitro* experiment. Additionally, the tumor tissues were immunohistochemically stained with anti-CD68 antibody to visualize macrophages in the tumor tissues (**Figure 12B**). The numbers of macrophages increased in both CD40p-treated and CD40p-CNP-treated tumor tissues. This indicates that the infiltration of macrophages into the tumors occurred following the CD40p or CD40p-CNP treatments. In conclusion, the intravenous injections of CD40p-CNP also demonstrated similar histological changes to the localized injections of CD40p into the tumors. The treatments directly induced the deaths of tumor cells and the recruitment of macrophages to the TME for the enhanced immunological response against tumors.

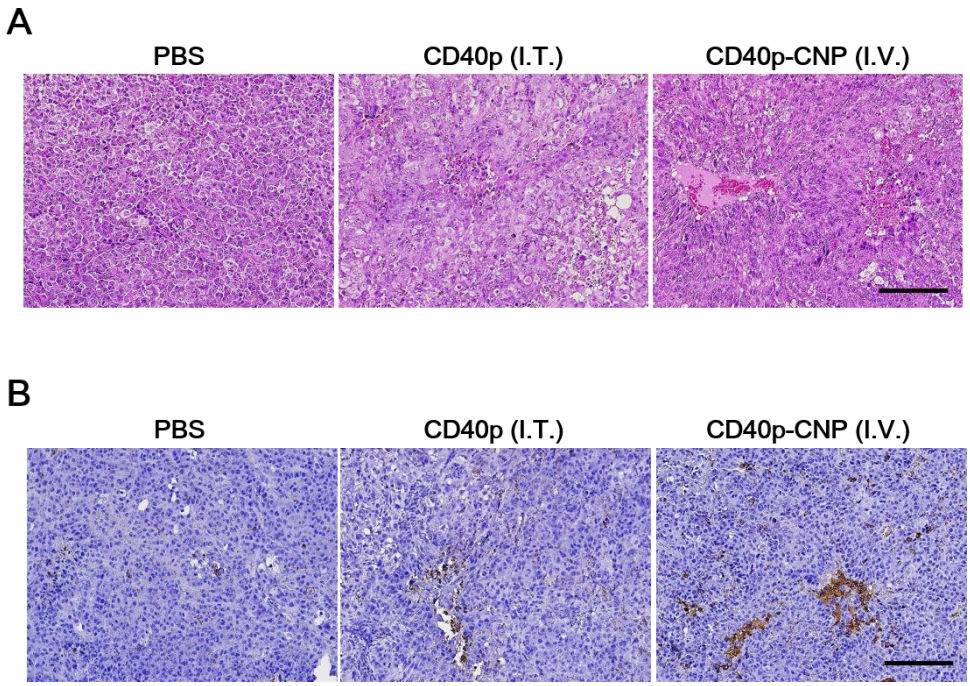

Figure 12. Histological analysis of the tumor tissues after the treatments with CD40p (I.T.), CD40p-CNP (I.V.), or PBS**.** (A) H&E staining (B) Anti-CD68 IHC staining against macrophages (brown) in the tumor tissues. Scale bar represents 200μm.

4. Conclusions

Localized delivery of immunotherapeutic agents to tumors and TME can alter the immunosuppressive nature of TME and re-educate the immune cells to either directly kill the tumor cells or promote inflammation for anti-tumor immune responses. For an effective tumor-targeted delivery, CD40-binding peptides, which bind to CD40 receptor on the surface of immune cells for their activation, were chemically conjugated with hydrophobically modified glycol chitosan nanoparticles that intrinsically accumulate in tumors following systemic injection. Results have shown the therapeutic effects of the nanoparticle that the binding of the peptide on the surface of the nanoparticle to the cell surface receptor triggered deaths of tumor cells and activation of macrophages for enhanced phagocytic activity. Systemic injection of the nanoparticles *in vivo* also produced similar results to the intratumoral injection of the CD40-binding peptides that significant inhibition of tumor growth was observed in both nanoparticle-treated and peptide-treated groups. This novel approach to cancer immunotherapy that utilizes nanoparticle to target tumor microenvironment and deliver immuno-modulating reagent for enhanced cell-mediated immune responses against tumor has a great potential in overcoming the immunosuppressive effects of TME. Combination of the nanoparticle with other signaling molecules for synergistic effects on immune cells or with chemotherapeutic reagents for more extensive destruction of tumors will also contribute to developing more effective treatment of cancer with minimal side effects.

5. References

[1] Lesterhuis WJ, Haanen JB, Punt CJ. Cancer immunotherapy--revisited. Nat Rev Drug Discov. 2011;10:591-600.

[2] Miller JF, Sadelain M. The journey from discoveries in fundamental immunology to cancer immunotherapy. Cancer Cell. 2015;27:439-49.

[3] Amoozgar Z, Goldberg MS. Targeting myeloid cells using nanoparticles to improve cancer immunotherapy. Adv Drug Deliv Rev. 2015;91:38-51.

[4] Kerkar SP, Restifo NP. Cellular constituents of immune escape within the tumor microenvironment. Cancer research. 2012;72:3125-30.

[5] Biswas SK, Mantovani A. Macrophage plasticity and interaction with lymphocyte subsets: cancer as a paradigm. Nature immunology. 2010;11:889-96.

[6] Tong AW, Stone MJ. Prospects for CD40-directed experimental therapy of human cancer. Cancer gene therapy. 2003;10:1-13.

[7] Elgueta R, Benson MJ, de Vries VC, Wasiuk A, Guo Y, Noelle RJ. Molecular mechanism and function of CD40/CD40L engagement in the immune system. Immunological reviews. 2009;229:152-72.

[8] Haanen JB, Schumacher TN. Vaccine leads to memory loss. Nature medicine. 2007;13:248-50.

[9] Quail DF, Joyce JA. Microenvironmental regulation of tumor progression and metastasis. Nature medicine. 2013;19:1423-37.

[10] De Palma M, Lewis CE. Macrophage regulation of tumor responses to anticancer therapies. Cancer Cell. 2013;23:277-86.

[11] Vonderheide RH. Prospect of targeting the CD40 pathway for cancer therapy. Clinical cancer research : an official journal of the American Association for Cancer Research. 2007;13:1083-8.

[12] Vonderheide RH, Glennie MJ. Agonistic CD40 antibodies and cancer therapy. Clinical cancer research : an official journal of the American Association for Cancer Research. 2013;19:1035-43.

[13] Murphy WJ, Welniak L, Back T, Hixon J, Subleski J, Seki N, et al. Synergistic anti-tumor responses after administration of agonistic antibodies to CD40 and IL-2: coordination of dendritic and CD8+ cell responses. Journal of immunology. 2003;170:2727-33.

[14] Gu L, Ruff LE, Qin Z, Corr M, Hedrick SM, Sailor MJ. Multivalent porous silicon nanoparticles enhance the immune activation potency of agonistic CD40 antibody. Adv Mater. 2012;24:3981-7.

[15] Rosalia RA, Cruz LJ, van Duikeren S, Tromp AT, Silva AL, Jiskoot W, et al. CD40-targeted dendritic cell delivery of PLGA-nanoparticle vaccines induce potent anti-tumor responses. Biomaterials. 2015;40:88-97.

[16] Mangsbo SM, Broos S, Fletcher E, Veitonmaki N, Furebring C, Dahlen E, et al. The human agonistic CD40 antibody ADC-1013 eradicates bladder tumors and generates T-cell-dependent tumor immunity. Clinical cancer research : an official journal of the American Association for Cancer Research. 2015;21:1115-26.

[17] Brunekreeft KL, Strohm C, Gooden MJ, Rybczynska AA, Nijman HW, Grigoleit GU, et al. Targeted delivery of CD40L promotes restricted activation of antigen-presenting cells and induction of cancer cell death. Molecular cancer. 2014;13:85.

[18] Dominguez AL, Lustgarten J. Targeting the tumor microenvironment with anti-neu/anti-CD40 conjugated nanoparticles for the induction of antitumor immune responses. Vaccine. 2010;28:1383-90.

[19] Buhtoiarov IN, Lum H, Berke G, Paulnock DM, Sondel PM, Rakhmilevich AL. CD40 ligation activates murine macrophages via an IFN-gamma-dependent mechanism resulting in tumor cell destruction in vitro. Journal of immunology. 2005;174:6013-22.

[20] Lum HD, Buhtoiarov IN, Schmidt BE, Berke G, Paulnock DM, Sondel PM, et al. Tumoristatic effects of anti-CD40 mAb-activated macrophages involve nitric oxide and tumour necrosis factor-alpha. Immunology. 2006;118:261-70.

[21] Beatty GL, Chiorean EG, Fishman MP, Saboury B, Teitelbaum UR, Sun W, et al. CD40 agonists alter tumor stroma and show efficacy against pancreatic carcinoma in mice and humans. Science. 2011;331:1612-6.

[22] Sandin LC, Totterman TH, Mangsbo SM. Local immunotherapy based on agonistic CD40 antibodies effectively inhibits experimental bladder cancer. Oncoimmunology. 2014;3:e27400.

[23] Rahimian S, Fransen MF, Kleinovink JW, Amidi M, Ossendorp F, Hennink WE. Polymeric microparticles for sustained and local delivery of antiCD40 and antiCTLA-4 in immunotherapy of cancer. Biomaterials. 2015;61:33-40.

[24] Park K, Kim JH, Nam YS, Lee S, Nam HY, Kim K, et al. Effect of polymer molecular weight on the tumor targeting characteristics of self-assembled glycol chitosan nanoparticles. Journal of controlled release : official journal of the Controlled Release Society. 2007;122:305-14.

[25] Kim K, Kim JH, Park H, Kim YS, Park K, Nam H, et al. Tumor-homing multifunctional nanoparticles for cancer theragnosis: Simultaneous diagnosis, drug delivery, and therapeutic monitoring. Journal of controlled release : official journal of the Controlled Release Society. 2010;146:219-27.

[26] Na JH, Koo H, Lee S, Min KH, Park K, Yoo H, et al. Real-time and non-invasive optical imaging of tumor-targeting glycol chitosan nanoparticles in various tumor models. Biomaterials. 2011;32:5252-61.

[27] Lee SJ, Min HS, Ku SH, Son S, Kwon IC, Kim SH, et al. Tumor-targeting glycol chitosan nanoparticles as a platform delivery carrier in cancer diagnosis and therapy. Nanomedicine. 2014;9:1697-713.

[28] Yoon HY, Son S, Lee SJ, You DG, Yhee JY, Park JH, et al. Glycol chitosan nanoparticles as specialized cancer therapeutic vehicles: sequential delivery of

doxorubicin and Bcl-2 siRNA. Scientific reports. 2014;4:6878.

[29] Khan S, Alonso-Sarduy L, Roduit C, Bandyopadhyay S, Singh S, Saha S, et al. Differential peptide binding to CD40 evokes counteractive responses. Hum Immunol. 2012;73:465-9.

[30] Edelhoch H. Spectroscopic determination of tryptophan and tyrosine in proteins. Biochemistry. 1967;6:1948-54.

[31] Chanput W, Mes JJ, Wichers HJ. THP-1 cell line: an in vitro cell model for immune modulation approach. International immunopharmacology. 2014;23:37-45.

[32] Daigneault M, Preston JA, Marriott HM, Whyte MK, Dockrell DH. The identification of markers of macrophage differentiation in PMA-stimulated THP-1 cells and monocyte-derived macrophages. PloS one. 2010;5:e8668.

[33] Koh E, Lee EJ, Nam GH, Hong Y, Cho E, Yang Y, et al. Exosome-SIRPalpha, a CD47 blockade increases cancer cell phagocytosis. Biomaterials. 2017;121:121-9.

[34] Genin M, Clement F, Fattaccioli A, Raes M, Michiels C. M1 and M2 macrophages derived from THP-1 cells differentially modulate the response of cancer cells to etoposide. BMC cancer. 2015;15:577.

[35] Mathur RK, Awasthi A, Wadhone P, Ramanamurthy B, Saha B. Reciprocal CD40 signals through p38MAPK and ERK-1/2 induce counteracting immune responses. Nature medicine. 2004;10:540-4.

[36] Chang H, Yhee JY, Jang GH, You DG, Ryu JH, Choi Y, et al. Predicting the in vivo accumulation of nanoparticles in tumor based on in vitro macrophage uptake and circulation in zebrafish. Journal of controlled release : official journal of the Controlled Release Society. 2016;244:205-13.

[37] Nam HY, Kwon SM, Chung H, Lee SY, Kwon SH, Jeon H, et al. Cellular uptake mechanism and intracellular fate of hydrophobically modified glycol chitosan nanoparticles. Journal of controlled release : official journal of the Controlled Release Society. 2009;135:259-67.

[38] Kuhn DA, Vanhecke D, Michen B, Blank F, Gehr P, Petri-Fink A, et al.

Different endocytotic uptake mechanisms for nanoparticles in epithelial cells and macrophages. Beilstein journal of nanotechnology. 2014;5:1625-36.

[39] Zanelli E, Toes RE. A dual function for CD40 agonists. Nature medicine. 2000;6:629-30.

[40] Dumas G, Dufresne M, Asselin E, Girouard J, Carrier C, Reyes-Moreno C. CD40 pathway activation reveals dual function for macrophages in human endometrial cancer cell survival and invasion. Cancer immunology, immunotherapy : CII. 2013;62:273-83.

[41] Jackaman C, Lew AM, Zhan Y, Allan JE, Koloska B, Graham PT, et al. Deliberately provoking local inflammation drives tumors to become their own protective vaccine site. Int Immunol. 2008;20:1467-79.

[42] Fransen MF, Sluijter M, Morreau H, Arens R, Melief CJ. Local activation of CD8 T cells and systemic tumor eradication without toxicity via slow release and local delivery of agonistic CD40 antibody. Clinical cancer research : an official journal of the American Association for Cancer Research. 2011;17:2270-80.

[43] Fransen MF, Cordfunke RA, Sluijter M, van Steenbergen MJ, Drijfhout JW, Ossendorp F, et al. Effectiveness of slow-release systems in CD40 agonistic antibody immunotherapy of cancer. Vaccine. 2014;32:1654-60.

요약 (국문초록)

종양미세환경 조절인자의 국소적 전달을 위한 펩타이드 글라이콜 키토산 나노입자 결합체 연구

암 면역치료법은 최근 몇 년 사이에 급부상하고 있는 암 치료 분야들 중 하나로, 우리 몸 안의 면역시스템을 이용하여 암과 대항 및 제어하는 데 초점을 둔 치료 방법이다. 호전적 성향의 CD40 단일 클론 항체를 이용한 암 면역 치료는 면역이 억제된 종양미세환경을 변화시킬 수 있는 여러 가지 메커니즘에 관여하여 항암 면역환경을 증진시킬 수 있는 새로운 치료방법으로 제안되고 있다. 이전 연구들에서 CD40 결합은 종양의 사멸을 유발할 뿐 아니라 대식세포들을 활성화시켜 재빠르게 종양에 침투하여, 종양을 제거하고 종양 기질의 감소를 촉진시킨다. 본 연구는, 항암 효과들을 유지함과 동시에 원치 않는 전제적인 부작용들을 피하기 위해서 CD40 결합 펩타이드를 소수성으로 변형시킨 글라이콜 키노산 나노입자와 결합시켜 CD40p-CNP를 만들고, 인간의 말초 혈액의 단핵 백혈구의 CD40 도메인을 일부분 모방한 호전적 성향의 CD40 결합 펩타이드를 종양과 종양미세환경으로 국소적 전달을 이뤘다. 세포 실험에서 면역 조절 나노 입자들은 인간의 암세포들에 대해 세포독성을 보였고, 대식세포의 식세포 작용을 증진시켰다. 종양 모델 마우스에 CD40p-CNP의 전신 주입했을 때 나노 입자들이 종양과 종양미세환경으로 표적 형으로 전달되었다. 그리고

상당한 종양 성장 억제 결과를 보였으며, 그 결과가 CD40 결합 펩타이드를 종양에 국소 주입한 결과와 유사하였다.

본 연구에서, 우리는 암 치료에서 종양기질을 표적하는 CD40 의존성 메커니즘을 통한 국소적 암 면역 치료의 잠재성을 입증하였다. 향후에 우리의 주요 연구 결과는 암 면역 치료에서 전신 주사를 통해 면역 치료제를 종양과 종양미세환경으로 국소적 전달하여 암을 면역 치료할 수 있는 새로운 방법을 제공할 수 있으며, 또한 항암치료제, 방사선 치료 등의 다른 암 치료 방법들과 병행 혹은 결합하여 치료했을 때 그 효과가 극대화 될 것으로 기대된다.

주요어 : 암 면역 치료, CD40 결합 펩타이드, CD40 항체, 종양미세환경, 키토산 나노 입자, 종양 침윤 림프구, 종양 성장 억제

학번 : 2015-21210